ON THE RELATION BETWEEN THE ELECTRON CONTENT OF THE IONOSPHERIC D-REGION, VARIATIONS OF THE RIOMETER ABSORPTION, AND THE H-COMPONENT OF THE GEOMAGNETIC FIELD

L.V.Zelenkova, V.A.Soldatov, J.V.Arkhipov, V.F.Laikova

Research Institute of Physics, Leningrad State University,
Stary Petergof, 198904, Leningrad, USSR.

The correlation between lower ionosphere disturbances, geomagnetic variations and radiowave absorption is one of the most actual problems of geophysics.

In this work we investigate the correlation between the electron density profile structure and riometer absorption, and between the absorption and the H-component magnetic field, in order to determine the relation between the [e]-profile parameters and the geomagnetic field variations.

1. To calculate theoretically the electron density behaviour during disturbed conditions from riometer absorption data, one can use the well-known formula: $[e]=\sqrt{q/\Psi}$, where q ($cm^{-3}s^{-1}$) is the ion production rate and Ψ ($cm^{3}s^{-1}$) is the effective loss rate.

PARTHASARATHY [1966] presents the relations between riometer absorption and the integral precipitating electron flux with E>40keV in the following form: $A(dB)=3.3\ 10^{-3}\sqrt{J(>40keV)}$.

ZELENKOVA [1988] showed that provided the integral precipitating electron flux has the power form as $J(>E)=k\cdot E^{-\gamma}$ we can find the flux parameters k and γ. For $\gamma=2$: $k=3{,}3^{-2}\ 10^{6}\ 40^{2}\ A^{2}$. Thus, for each value of riometer absorption, it is possible to obtain the differential precipitating electron flux responsible for it.

Then we obtain the ion production rate using the formula from paper by KHVOROSTOVSKIY [1987].

2. To determine the height profile of [e], the investigations of effective loss rate variations were made using the published data referenced in the paper by GLEDHILL [1986]. All the height profiles were separated into 4 groups:

1) Ψ_1 height profiles for the day-time quiet conditions (12 profiles),
2) Ψ_2 height profiles for the night-time quiet conditions (7 profiles),
3) Ψ_3 height profiles for the day-time disturbed conditions (13 profiles),
4) Ψ_4 height profiles for the night-time disturbed conditions (5 profiles).

Mean profiles for 4 types of conditions are shown in Fig.1. The value of the disturbed (both day-time and night-time) effective loss rate is less than the quiet one as seen from Fig.1 even taking into account the considerable error (shown). The fact of dependence of the effective loss rate on ionospheric disturbance level was established in the paper by ZELENKOVA [1981]. Using a 3-ion D-region model for the height range of $\lambda=[M^{-}]/[e]>1$, the analythical dependence was derived also in that paper.

Because the formula from paper by ZELENKOVA [1981] is correct when $\lambda>1$, we used also a combined profile of Ψ, where effective loss rate was calculated for the heights from 50km to the height where Ψ becomes equal to $2\ 10^{-7}\ cm^{3}s^{-1}$, and such a value of Ψ was assumed up to h=95km. In the height range 95-120km Ψ varied uniformly from $2\cdot10^{-7}$ to $2\cdot10^{-8}\ cm^{3}s^{-1}$ [ADAMS,1965].

3. The experimental rocket profiles of the electron density were taken from the work of MIYAZAKI [1978] in form of a catalogue [NESTEROVA,1985]. To compare the calculated and the experimental profiles, we chose the parameter

$$\Delta\omega=([e]_c-[e]_m)/[e]_c \qquad (1)$$

where $[e]_c$ is the calculated electron concentration and $[e]_m$ is that measured during the rocket ascent.

Moreover, the availability of both ascent and descent rocket electron

density profile data allowed us to estimate a similar parameter:

$$\Delta\omega = ([e]_a - [e]_d)/[e]_a \qquad (2)$$

where $[e]_a$ is the electron density corresponding to the fixed height during the rocket ascent, $[e]_d$ being that obtained during the rocket descent.

Tab.1 shows the absolute values of parameters $|\overline{\Delta\omega}|$ and $|\overline{\Delta\omega_i}|$.

The estimation of $\Delta\omega$ was performed with Ψ_4 (mean night-time disturbed conditions profile, abbreviated as NGN in Tab.1) using combined Ψ profile (abbreviated as NGT in Tab.1) for the riometer absorption between 0.3 and 5dB.

4. Experimental profiles of [e] from the paper by MIYASAKI [1978], complemented with those from PFISTER [1967] and DERBLOM [1973] were analysed by ZELENKOVA [1982] by using four parameters which characterise the [e]-profile structure of the disturbed D-region. These are h_1 - height of 10^2 cm^{-3} electron appearance, h_2 - height of strong enhancement of [e]-gradient and N_2 - concentration of the "step" bottom, N_3 - concentration of electrons at h=95km. Tab.2 shows the variation of the above mentioned parameters versus riometer absorption between 0.3 and 5 dB.

5. Generally accepted parameter that reflects magnetic field variation during geomagnetic disturbances is the AE-index.

We attempt to connect the electron density profile parameters with the AE-index.

Profiles were compiled from the catalogue of MCNAMARA [1978] and also from the catalogue of NESTEROVA [1985], where they are given in a digital form. Only the auroral zone profiles during disturbances were selected, which corresponds to the indexes 9-13 [NESTEROVA,1985; MCNAMARA,1978].

Thus, 44 profiles for night-time conditions were chosen.

All the profiles were selected into different groups according to the AE-index value in the following manner: $0 < AE < 100$(6), $100 < AE < 200$(9), $200 \leqslant AE < 300$(8), $300 \leqslant AE < 400$(8), $400 \leqslant AE < 500$(7), $500 \leqslant AE < 600$(2). $AE \geqslant 600$(4).

Attention was paid to geographic location of stations: Andoya(69.3°N, 16°E)(25), Syowa(69.5°S,39°E)(11), College(64.9°N,212°E), Churchill(58.8°N, 265.8°E)(2) (the number of profiles is in the brackets).

Parameters that characterise the electron density distribution in the D-region are the heights of appearance of the electron density equal to 10^2 cm^{-3}, 10^3 cm^{-3}, 10^4 cm^{-3}, respectively.

Mean profile of the electron density distribution was calculated (Tab.3).

6. To compare the electron density variations obtained using AE-index with 4-parameter model (see part 4), we study the relations between the riometer absorption and AE-index. We got the ionospheric data from Finnish Academy of sciences and compared them with AE-index. We explore the data from 1978-1979 years. Two intervals were chosen: 19-22^{h}LT and 23-01^{h}LT. Such dependences are shown in Fig.2 for the stations Kevo and Sodankyla. One can conclude from the Fig.2:

1)the absorption for the night-time (23-01^{h}LT) is greater for farther to the south station (for the same AE-index);

2)both for Kevo and Sodankyla the riometer absorption is greater at 23-01^{h}LT than 19-22^{h}LT.

Using Fig.2, it is easy to obtain the riometer absorption for each value of AE-index.

Tab.3 summarises the results from Fig.2 and from the catalogue. The designations are: AE is the AE-index in γ, N is the number of profiles, A,dB is the magnitude of the riometer absorption; $h(N_{10^2})$, $h(N_{10^3})$, $h(N_{10^4})$, are the heights of appearance of the appropriate electron density.

Conclusions from the data of Tab.1, 2 and 3 :

1. Theoretical investigations allow us to determine the height distribution of [e] with relative error less than 100%. At the same time, the experimental measurements are subject to relative error (ascent and descent) as large as 50%. That reflects a wide variability of auroral ionosphere, rather then imprecision of the experiment.

2. Both experimental and theoretical investigations shows the enhancement of riometer absorption due to:

a) the appearance of equilibrium electron density about 10^2 cm^{-3} at heights h<50km (lower part of D-region),

b) the increase of [e] by more than an order of magnitude in the upper part of the D-region (h>90km).

Parameter h_1 characterize the hardness of electron flux spectrum, while the parameters N_2 and N_3 characterize the intensity of the flux.

As seen from Tab.2,3 the best accordance between the experimental and calculated (restored) parameters of [e]-profile appears. The discrepancy between the h_{1m} and h_1 (19-22), h_1 (23-01) is explained by the fact that the station becomes situated northward of the precipitation zone during the large values of AE-index.

REFERENCES

Adams G.W., Masley A.J. Production rates and electron densities in the lower ionosphere due to Solar cosmic rays. J.Atm.Terr.Phys.,27,289,1965.

Derblom U., Ladell L. D-region parameters at high latitudes obtained from rocket experiments. J.Atm.Terr.Phys.,35,2123,1973.

Gledhill J.A. The effective recombination coefficient of electrons in the ionosphere between 50 and 150 km. Radio Sci.21,399,1986.

Khvorostovskiy S.N., Zelenkova L.V. Geomagn.and aeron.,27,599,1987(in Russian).

McNamara L.F. Ionospheric D-region profile data base. Report UAG-67,1978.

Mechtly E.A., Bowhill S.A., Smith L.G. Changes of lower ionosphere electron concentrations with solar activity. J.Atmosph.Terr.Phys.34,1899,1972.

Miyazaki S. Ionospheric plasma probe studies and ionospheric structure studied by space vehicle observations. J.Radio Res.Lab.25,153,1978.

Nesterova I.I., Ginsburg E.I. Catalog of D-region electron density profiles of the ionosphere. Novosibirsk,1985(in Russian).

Parthasarathy R., Berkey F.T., Venkatesan D. Auroral zone electron flux and its relation to broadbeam radiowave absorption. Planet.Space Sci.14,65,1966.

Pfister W. Auroral investigations by means of rockets. Space Sci.Rev. 7,642,1967.

Zelenkova L.V. Dissertation,1981(in Russian).

Zelenkova L.V. D-region electron density distribution. Geomagn.Res. N 14,101,1976.

Zelenkova L.V. Structure of the electron density profile during auroral disturbances. Magnetosph.res.N 1,187,1982(in Russian).

Zelenkova L.V., Soldatov V.A. Restoration of the impinging electron differential fluxes from riometric absorption. Magnetosph.res.N 11,133,1988 (in Russian).

TABLE 1

h, km	$\lvert\overline{\Delta\omega}\rvert$ (NGT)	$\lvert\overline{\Delta\omega}\rvert$ (NGN)	$\lvert\overline{\Delta\omega_i}\rvert$
70	0.47	0.62	0.59
75	0.47	0.70	0.45
80	0.44	0.34	0.50
85	0.68	0.76	0.60
90	0.53	0.75	0.47
95	0.85	0.98	0.36
100	1.12	0.99	0.40

TABLE 2

A, dB	h_{1m}, km	h_{1c}, km	h_2, km	N_2, cm^{-3}	N_{3m}, cm^{-3}	N_{3c}, cm^{-3}
0.3	68	65	78	3 10	3 10	4 10
0.5	60	56	80	10	7 10	6 10
1.2	58	55	83	2.5 10	8 10	10
1.3	57	-	82	2 10	10	-
1.5	58	55	83	10	3 10	2 10
2.6	55	52	75	8 10	4 10	3 10
5.0	55	50	-	-	5 10	6 10

TABLE 3

$\langle AE, \gamma \rangle$	N	A, dB (19-22)	A, dB (23-01)	h_{10^2}, km	h_{10^3}, km	h_{10^4}, km
0 - 100	6	0.2	0.4	64±9	74±4	83±4
100 - 200	9	0.5	0.7	62±2.2	72±5	82±5
200 - 300	8	0.9	1.2	50±8	67±6	80±2
300 - 400	8	1.3	1.7	63±5.5	73±3.5	80±3
400 - 500	7	1.5	2.5	79±8	79±8	87±8
500 - 600	2	2.0	3.0	83±3	89±1	96±4
> 600	4	2.3	4.0	67±5	65±5	75±5

Fig 1

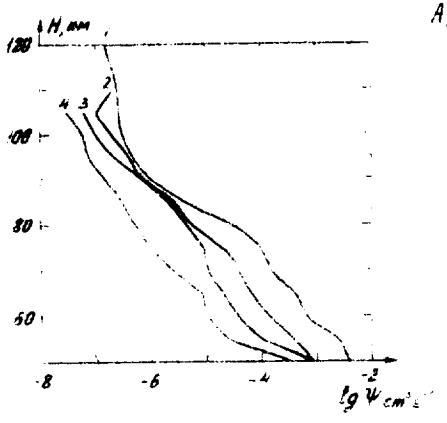

Fig 2